Supporting Information to

Oxygen and Lithium Doped Hybrid Boron-Nitride/Carbon Networks for Hydrogen Storage

Farzaneh Shayeganfar[1,2] and Rouzbeh Shahsavari[1,3,4,*]

[1]Department of Civil and Environmental Engineering, Rice University, Houston, TX 77005

[2]Institute for Advanced Technologies, Shahid Rajaee Teacher Training University, 16875-163, Lavizan, Tehran, Iran.

[3]Department of Material Science and NanoEngineering, Rice University, Houston, TX 77005

[4]Smalley Institute for Nanoscale Science and Technology, Rice University, Houston, TX 77005

*Corresponding author email: rouzbeh@rice.edu

This Supporting Information is divided into three parts:

SI. System setup for creating the pillared structures

SII. Continuum model for adsorption of hydrogen molecule on pillared GBN

SIII. Conclusion

SI. System Setup

In this paper, we employ first-principles calculations to probe the stability of hybrid pillar graphene (PG) with BNNT junction via the covalent attachment. The main outline of this study is to establish a basic physical picture of junction construction between a BNNT and graphene that covalent bonds between them create some ripples in graphene and also distort the BNNT geometry. Since graphene

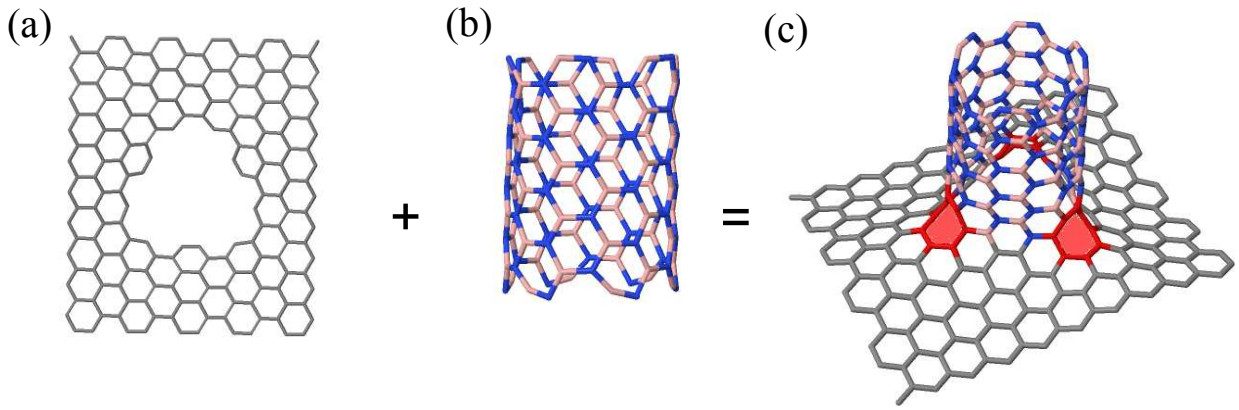

FigS1. (a) Scheme of the octagon molecular junction of graphene, (b) (6,6) BNNT, (c) Graphene-BNNT octagonal junction.

induces a partial sp^3 into the sp^2 network of (6,6) tube, it opens up a band gap for graphene and for the semiconductor (6,6) BNNT, the sp^3 hybridization between the graphene and nanotube induces impurity states on the Fermi level. [S1]

Our study is started with the built supercell, which had the removed carbon atoms from the center and suitable for placing an armchair (6,6) BNNT at the center hole (Figure S1), based on the first-principles, density functional theory within the framework of the SIESTA package.

Fig. S2a,b show a schematic picture of 3D PBN and PGBN made BNNT and 2D monolayer graphene sheets with octagonal junction. However, all possible configuration (heptagonal and octagonal, ...) should satisfy Euler's theorem of polygons,[S2,S3] which allows determining the bond surplus. For carbon-based materials, large number of possibilities with different number of sides and sizes of rings exist to form seamless sp^2 structure, however, in the case of hybrid BN structures with alternating B and N atoms and sp^2 configuration, only rings with an even number of sides are feasible[S2] (e.g., Fig. S1b, shows a schematic picture of pillar graphene made of 1D BNNT with 3 sides).

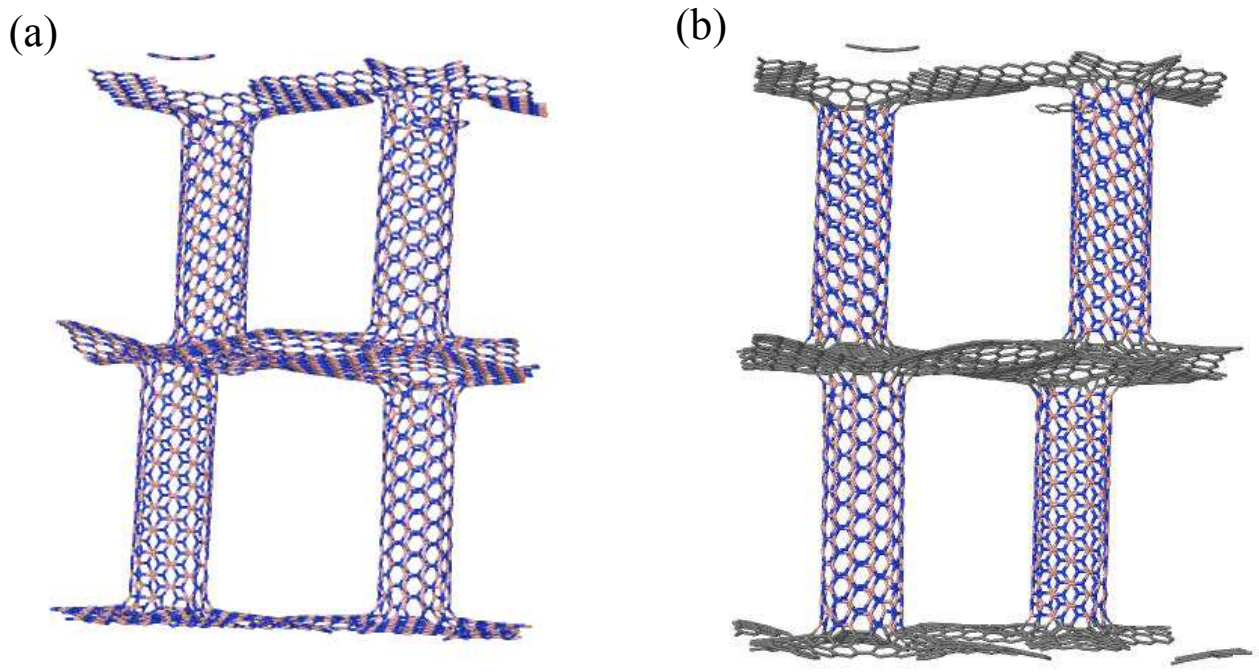

Fig S2. (a) Scheme of the (a) pillared BNNT (PBN) and (b) pillared GE+BNNT (PGBN).

SII. Continuum Model for Adsorption of Hydrogen Molecules on Pillared BN and Pillared GBN

In this paper, we use the continuum model and an equation of states to investigate the storage of hydrogen molecules inside PGBN frameworks, which consists of two parallel graphene nanosheets separated by perpendicular BNNT as columns. As mentioned in section 2.3 in the main text, the weak interactions between atoms in our nanopillar framework take to account using the LJ potential, U (ρ):[S4]

$$U\,(\rho) = 4\varepsilon\,[(\frac{-\sigma}{\rho})^{6} + (\frac{\sigma}{\rho})^{12}] = \left(\frac{-A}{\rho^{6}}\right) + \left(\frac{B}{\rho^{12}}\right) \qquad \text{(S1)}$$

where ρ, denotes the distance between two atoms and A and B are attractive and repulsive Hamaker constants, respectively. We employed the continuum approach utilized by Cox et al.[S5,S6], while the BN nanotube simulated as a hollow and continuous cylinder and the graphene represented as a surface. In this approach, the continuum energy (E_C) is given by:[S7]

$$E_C\,(\Re,z) = \alpha \int_{S_1} U(\rho)dS_1 + \sum_{i=1}^{3} \alpha_i \int_{S_2} U(\rho)dS_2 \qquad \text{(S2)}$$

where α, α_i are the atomic number density of the graphene sheet, i=1 for hydrogen, i=2 for boron and i=3 for nitrogen on the cylindrical surface, and dS_1 and dS_2 denote the surface element of the graphene sheet, and the cylinder, respectively. It is analytically convenient to approximate the graphene sheet by a circular disc, to take $dS_1 = 2/\pi\ R\ dR$. The schematic diagram for the proposed system is also shown in Figure S3.

The integrals over surface elements of dS_1 and dS_2 are done analytically by employing Mathematica software. With these assumptions, the total potential energy of the system becomes: [S7]

$$E_C(\Re, z) = \alpha\,\pi\left[-\frac{A}{2}\left(\frac{1}{z^4}-\frac{1}{(L-z)^4}\right)+\frac{B}{5}\left(\frac{1}{Z^{10}}+\frac{1}{(L-Z)^{10}}\right)+\frac{A}{2}\left(\frac{1}{(Z^2+\Re^2)^2}+\frac{1}{((L-z)^2+\Re^2)^2}\right)-\right.$$

$$\left.\frac{B}{5}\frac{A}{2}\left(\frac{1}{(Z^2+\Re^2)^2}+\frac{1}{((L-z)^2+\Re^2)^2}\right)\right]+\sum_{I=1}^{4}\frac{3\pi\alpha S}{8}\left[\begin{array}{c}-\frac{2A_i\,\pi}{(S-\Re)^5}\,F\left(\frac{5}{2},\frac{1}{2};1;-\frac{2\Re S}{(S-\Re)^2}\right)+\\ \frac{21B_i\,\pi}{16(S-\Re)^{11}}\,F\left(\frac{11}{2},\frac{1}{2};1;-\frac{2\Re S}{(S-\Re)^2}\right)\end{array}\right] \quad \text{(S3)}$$

where z denotes the distance between the hydrogen and the lower graphene sheet, L the separation between the two graphenes, $\Re$ and S the radial distance in the planes of the graphene sheets and the approximate radius of the graphene sheet, respectively (Figure S3).

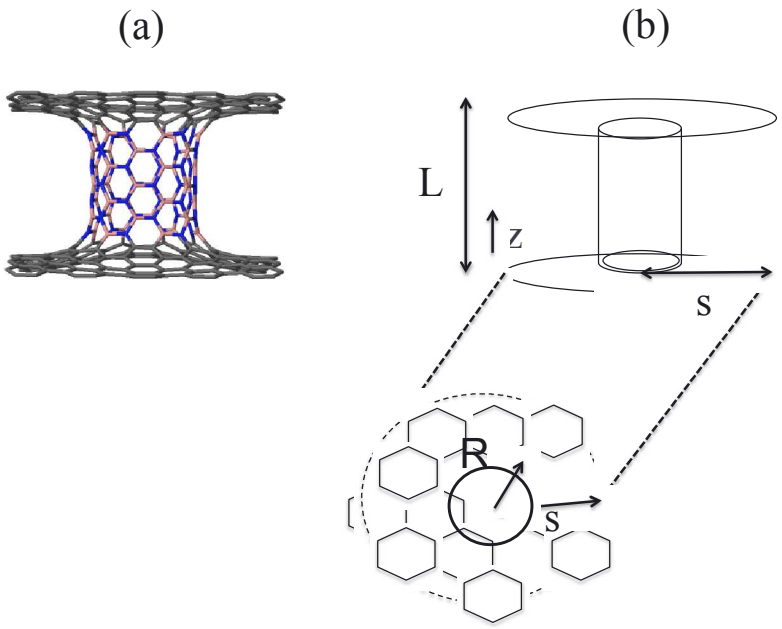

Fig S3 . Schematic plan for continuum model of PGBN hydrogen storage.

In addition, (A, A_i) are the attractive constant for H_2–graphene, H_2–(i=B,N) atom at the pillars. (B, B_i) denote the repulsive constant for H_2–graphene, H_2–(i=B,N) atom at the pillars and F is the hypergeometric function.[S8] The values of all parameters used for computation are brought in Table S1.

TABLE S1. Numerical values for A, B, A_i and B_i using the Lorentz-Berthelot mixing Rule[S7]. $\left(U(\mathrm{r}) = \left(\frac{-\mathrm{A}}{\mathrm{r}^6}\right) + \left(\frac{\mathrm{B}}{\mathrm{r}^{12}}\right)\right)$

Description	Parameter	Value
Attractive constant H_2 graphene	A	9.61 $Å^6$
Repulsive constant H_2 graphene	B	8695.5 $Å^{12}$
Attractive constant H_2-B	A_1	13.14 $Å^6$
Repulsive constant H_2-B	B_1	12394.74 $Å^{12}$
Attractive constant H_2-N	A_2	17.20 $Å^6$
Repulsive constant H_2-N	B_2	13899.03 $Å^{12}$
Attractive constant H_2-C	A_3	13.531 $Å^6$
Repulsive constant H_2-C	B_3	12493.01 $Å^{12}$
vdW radius for H_2	r_{ij}	1.51 Å

The probability of finding hydrogen in two states, the bulk gas phase or the adsorbed phase inside the nanopillar, can be determine as $P_{ads}(\Re, z) = 1-\exp(-|E(\Re,z)| / k_BT)$,[S9] where k_B is Boltzmann's constant and T is the temperature.

The equations of state for two different states, the adsorbed and the bulk gas phase are given by the equations:

$$P\left(\frac{V_{ads}}{n_{ads}} - v\right) = RT\exp\left(\frac{-Q}{RT}\right), \qquad P\left(\frac{V_{bulk}}{n_{bulk}} - v\right) = RT \qquad \text{(S4)}$$

where P is the external pressure, V_{ads} is the adsorption volume ($V_{ads} = \int_{V_1} P_{ads}(\Re, z)\, dV$), n_{ads} is the number of moles of adsorption phase, v is the occupied molar volume of gas molecules, R is the molar gas constant, Q is the heat of adsorption ($Q = |E_{avg}| + k_B T/2$), V_{bulk} is the bulk volum ($V_{bulk} = \int_{V_{free}}[1 - P_{ads}(\Re, z)]\, dV$) and n_{bulk} is the number of moles of bulk gas phase. The average interaction energy is defined as:

$$E_{avg} = (\int_{V_f} Ec(\Re, z)\, dV)/ V_f \qquad (S5)$$

To make the numerical calculations physically reasonable, we terminated the numerical iterations wherever ($P > \frac{|E_{avg}|-(K_B T/2)}{V}$) and ($n > \frac{3S^2 D}{4 r_H^3 N_A}$) is satisfied ($n = n_{ads} + n_{bulk, rH}$ denotes the van der Waals radius[S10] and N_A is Avogadro's constant). These two conditions indicate that hydrogen molecules are trapped inside the pillars while the work by external pressure on the hydrogen molecule plus its kinetic energy is smaller than its binding energy.[S10]

Continuum results

Upon substituting the corresponding parameters into equation S3 without the summation terms, the total potential energy E_C of a hydrogen molecule placed between PGBN can be obtained, which is plotted in Figure S3. We conclude that the total potential energy decreases in the R direction, which reflects the short interaction range for van der Waals forces and confirms our results with atomistic and molecular dynamic simulations. As we can see in Figure S4a, for z~0-L, the interaction between the hydrogen molecule and pillared structure is enhanced. Moreover, the potential energy for the region close to inner hole (octagonal junction) is greater than the potential energy at the edges (Figure S4b).

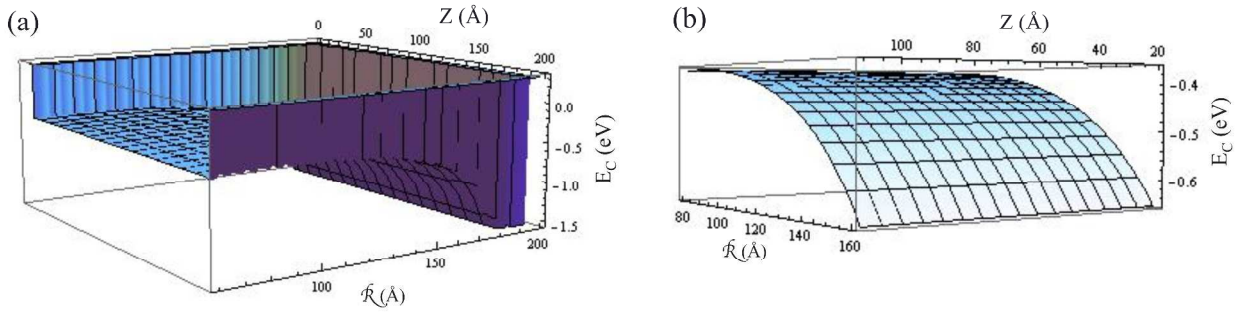

Fig S4. (a) Total potential energy ($E_C(R,z)$), which are related to the continuum model (Eq. (S4)) for hydrogen stored between two parallel graphene sheets and BNNT with L = 20 nm, where E_C is in eV and z and R are in Å. For z ~ 0, L, interaction between hydrogen molecule and pillared structure is enhanced. (b) The potential energy for ($R > S_0$) region, where S_0 is radius of inner hole (Figure S3b), is enhanced close to inner hole.

Finally, using equation S4, we obtain the gravimetric hydrogen uptake of hydrogen for PGBN and PBN, which is given in Figure S5. The numerical results for hydrogen uptake between graphene sheets and BNNT increase monotonically from 0 wt% to 9.3 wt% and for PBN the hydrogen uptake values increase up to 8.1 wt%, which is in agreement with our results in the main paper.

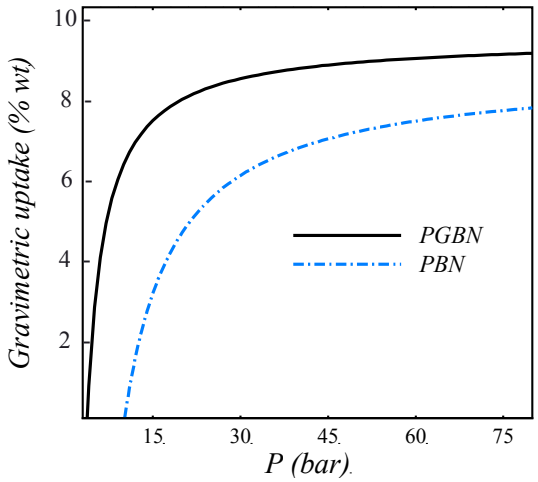

Fig S5. Gravimetric hydrogen uptakes for PGBN and PBN at 77 K and pressure up to 80 bar.

SIII. Conclusion

One of the characteristics that differentiate PBN and PGBN from other hydrogen storage materials is the richness of factors that influence their hydrogen uptake capacity. The first notable characteristic of porous pillared materials is surface area and pore volume, which have positive effect on hydrogen

storage. The other characteristic for enhancement of hydrogen capacity is chemical doping of porous material.

SUPPORTING REFERENCES

[S1] F. Shayeganfar and R. Shahsavari, Electronic and Pseudomagnetic Properties of Hybrid Carbon/Boronnitride Nanomaterials via Ab-initio Calculations and Elasticity Theory Carbon, **2016**, 99, 523-532.

[S2] N. Sakhavand, R. Shahsavari, Synergistic Behavior of Tubes, Junctions, and Sheets Imparts Mechano-Mutable Functionality in 3D Porous Boron Nitride Nanostructures R. J. Phys. Chem. C, **2014**, 118, 22730-22738.

[S3] P. R. Cromwell, Polyhedra; Cambridge University Press: New York, **1997**.

[S4] J. E. Jones, On the determination of Molecular Fields. II. From the equation of State of a Gas, Proc. R. Soc. A **1924**,106, 441.

[S5] B. J. Cox, N. Thamwattana and J. M. Hill,Proc. Mechanics of Atoms and Fullerenes in Single-Walled Carbon Nanotubes. I. Oscillatory Behaviors, *R. Soc. A* **2007** 463, 461.

[S6] B. J. Cox, N. Thamwattana and J. M. Hill,Proc. Mechanics of Atoms and Fullerenes in Single-Walled Carbon Nanotubes. II. Oscillatory Behaviors, *R. Soc.* A **2007** 463, 477-494.

[S7] Y. Chan and J. M. Hill, Hydrogen Storage Inside Graphene-Oxide Frameworks. *Nanotechnology* **2011**, 22, 305403, 8.

[S8] M. Stone and P. Goldbart **2009** Mathematics for Physics: A Guided Tour for Graduate Students (Cambridge: Cambridge University Press).

[S9] Thornton A W, Nairn K M, Hill J M, Hill A J and Hill M R, Metal-Organic Frameworks Impregnated with Magnesium-Decorated Fullerenes for Methane and Hydrogen Storage, J. Am. Chem. Soc. **2009** 131 10662–9.

[S10] S. S. Batsanov, Van der Waals Radii of Hydrogen in Gas-Phase and Condensed Molecules, *Struct. Chem*. **1999**, 6, 395–400.